Toward the relationship between local quantum Fisher information and local quantum uncertainty in the presence of intrinsic decoherence

Fadwa Benabdallah[1], **Khadija El Anouz**[2,a] , **Mohammed Daoud**[3,4]

[1] LPHE-Modeling and Simulation, Faculty of Sciences, Mohammed V University in Rabat, Rabat, Morocco
[2] Laboratory of R&D in Engineering Sciences, Faculty of Sciences and Techniques Al-Hoceima, Abdelmalek Essaadi University, Tétouan, Morocco
[3] ICTP, Strada Costiera 11, 34151 Trieste, Italy
[4] Department of Physics, Faculty of Sciences, University Ibn Tofail, Kenitra, Morocco

Abstract The delicate relationship between the concepts of local quantum uncertainty, local quantum Fisher information and concurrence is investigated. This is analyzed by quantifying the non-classical correlations inherent in a two-qubit XXZ open system interacting with its surrounding environment in the presence of an external magnetic field. The second part of this work investigates different kinds of states, namely pure, Werner, mixed, and maximally entangled states via solving the time-dependent Milburn equation. Indeed, by controlling various interaction parameters, it is shown that the non-classical quantifiers and entanglement witness by means of local quantum uncertainty, local quantum Fisher information, and concurrence, respectively, fluctuate approximately similarly between their maximum and minimum bounds, where in general the sudden death, sudden birth, oscillations, and frozen correlations phenomena appear in the case of Werner and maximally entangled states. Finally, a scheme of quantum teleportation protocol is proposed in order to make a comparative study between teleported non-classical correlations and entanglement under the influence of the intrinsic decoherence phenomenon.

1 Introduction

The characterization as well as the quantification of quantum correlations in composite quantum systems have been considered in different areas of quantum information science [1–3] as for instance in quantum computation and quantum estimation theory and stimulated interesting works [4–8]. Now, it is commonly accepted that quantum correlations constitute a key resource in the process of the implementation of various quantum protocols, including: quantum teleportation [8–10], quantum cryptography [11], quantum sensing [12], etc. In this sense, tools were developed in the last two decades to quantify the entanglement rate inherent in a quantum state [13–16]. The most popular one is the concept of the concurrence introduced by Wootters [4,13,17]. Another tool recently introduced in the literature is the concept of the so-called Local Quantum Uncertainty (LQU) that is now considered a reliable tool to quantify quantum correlations in multipartite quantum systems [18,19]. Roughly speaking LQU is investigated as a non-classical correlations quantifier of a multipartite quantum system [19]. It was introduced first time by Girolami et al [18] using the information of the Wigner Yanase Skew information [20]. Indeed, the LQU is originally defined as the minimum of skew information and it is another type of discord-like quantifiers of the uncertainty presented in a quantum state according to its non-commutativity using local observables [18,19,21]. Interestingly enough, the LQU is related directly to the notion of quantum Fisher Information (QFI) and Local quantum Fisher Information (LQFI) and gives an important link between quantum information theory and quantum estimation theory [22–24]. Indeed, it has been shown that quantum Fisher information provides a measure to investigate the entanglement for multipartite entangled systems [25]. Recently, LQFI has been suggested as a very successful tool to quantify quantum correlations in a composite quantum system [26,27]. In fact, the investigation and characterization of LQFI is performed using the optimization over all the observables of one of the subsystems of the whole composite system [26,27]. However, since both quantities, namely LQU and LQFI basically, depend on the quantum uncertainty concept, it might be used as good non-classical correlations quantifiers that satisfy all the conditions needed to be a reliable a measure of quantum correlations [28].

In recent years, the open quantum systems theory have acquired growing importance within the field of quantum information. Indeed, it is at the heart of many physical concepts used to understand and manipulate the interaction between a quantum system and its environment. On the other hand, the interaction of an open quantum system with its surrounding environment as a single composite system can be approached using concurrence, LQU, and LQFI as non-classical quantifiers in order to examine the correlations between its components. Indeed, an open quantum system exhibits the decoherence phenomenon which has been examined for different types of interaction in the literature [29–31]. Indeed, many works paid attention to study non-classical correlations by

---

[a] e-mail: elanouzkhadija1994@gmail.com (corresponding author)

means of LQU and QFI and examined the dynamics of open systems interact with their environments [27,32–35]. For example, L-P. Chen et al [36] examined the dynamics of LQU and LQFI for a two-qubit system driven by a classical phase noisy laser and they showed that for an open quantum system, the LQU is bounded by LQFI. Similar analyses were reported by B-L. Ye who examined the LQFI as a non-classical correlations quantifier in order to study the quantum phase transition in a spin-1/2 XX Heisenberg chain with three spin interactions [37]. Moreover, M. Ali studied the LQU for a multipartite system and proposed an analytical formula to derive the LQU in multipartite case [19]. Finally, V. Abhignan et al studied a two-qubit spin squeezing model in order to compare the LQU with other quantifiers of quantum correlations, namely trace distance discord and uncertainty-induced quantum nonlocality [33]. They concluded that the entanglement suffers from intrinsic decoherence and exhibits a sudden death phenomenon, while the non-classical quantifiers are more robust against intrinsic decoherence.

The spin-chain frameworks are exemplary systems used to investigate a wide range of physical systems, and various potential applications in quantum information, including: quantum phases, quantum communication, phase transitions, etc. Recently, a particular interest has been devoted to physically understand the Heisenberg spin chain models with Dzyaloshinski–Moriya interaction. For example, in Ref. [38], the authors have used this coupling as a good marker of quantum phase transitions. Moreover, this model is successfully appointed to generate entangled network from partially entangled states, thermal entanglement, teleportation fidelity, and dense coding [39,40]. In particular, the spin chains have acquired an attractive attention within the area of quantum information processing. Indeed, such spin chain has been devoted to investigate quantum data transmission through microscopic distances via considering them as a powerful states used to transfer information between two sites that ensure the building of quantum buses used to connect different computer components [41]. The core idea underlying the first part of this work is to study the dynamics of quantum correlations under intrinsic decoherence [42]. We consider a two-qubit XXZ Heisenberg spin chain subjected to an inhomogeneous magnetic field. We shall employ LQU and LQFI to quantify the quantum correlations in the quantum system, and we shall also use the concurrence as a witness tool to discuss the non-separability. In particular, we examine four different kinds of states, namely pure, mixed, maximally entangled, and Werner states [43]. The last class of states are significant in quantum information and computation processing because they are able to ensure the separability of mixed states since they have been classified as the generalized maximally entangled mixed states [43]. We shall evaluate the joint qubit–qubit state quantum correlations by means of concurrence, local quantum uncertainty, and local quantum Fisher information under the intrinsic decoherence effect. It is shown that these quantities fluctuate approximately in the same manner between their maximum and minimum amplitudes, where we have studied different phenomena, including sudden death, sudden birth, oscillations, and frozen correlations phenomena. The dynamical evolution of these quantities depends basically on the interaction parameters and appears fast in the case of Werner and mixed states. In the second part of this work, we shall focus our attention to quantum teleportation process which is the transmission of the information encoded in an unknown state from a sender named conventionally Alice to another located receiver, Bob using classical and quantum channels [8] . To implement this process of quantum teleportation, we evaluate quantum correlations, by means of LQU and LQFI and entanglement in terms of the concurrence of the final teleported state. Indeed, one of the most challenges of this work is given in the possibility to create and examine local quantum correlations between the proposed open system and its environment. According to this, we shall investigate the impact of the decoherence phenomenon on quantum teleportation protocol. Finally, we examine the fidelity in order to exhibit the credibility of transmitting the unknown state.

The paper is organized as follows. In Sec.2 , we give the Hamiltonian proposed two-qubit Heisenberg XXZ model and the corresponding density operator derived from the exact solution of time-dependent Milburn equation. In Sec.3, we review the definitions and the properties of concurrence, LQU, and LQFI. Their dynamics behaviors versus the interaction parameters for different proposed initial quantum states are considered in Sec.4. By using the standard teleportation protocol, the output state of the two-qubit entangled state is investigated in Sec.5. The evaluation of the fidelity, average fidelity, and the non-classical correlations of teleported state or output state is given in Sec.6 . Finally in Sec.7, we conclude with a summary and some future directions.

2 Theoretical model

2.1 Two-qubit Heisenberg XXZ model

Consider a bipartite quantum system, namely a Heisenberg XXZ spin-1/2 chain interacting with an external magnetic field, B with only nearest-neighbor interactions. The Hamiltonian of this system is given as below

$$H = J(s_1^x s_2^x + s_1^y s_2^y) + \Delta s_1^z s_2^z + (B - b)s_1^z + (B + b)s_2^z. \tag{1}$$

The coupling J describes the spin interaction strength, being anti-ferromagnetic when $J > 0$ while is ferromagnetic when $J < 0$. B is the external magnetic field applied in the z-direction, while b denotes the degree of inhomogeneity of the field. Δ is the exchange anisotropy parameter. For $\Delta = 0$, the model reduces to the isotropic XX, while for $\Delta = J$, the model is simply the isotropic Heisenberg XXX model. The Heisenberg spin-1/2 operators s_i^α ($\alpha = x, y, z$) are expressed in terms of the familiar Pauli matrices σ_i^α, acting on qubit i, as $s_i^\alpha = \hbar \sigma_i^\alpha / 2$. For sake of simplicity, we set $\hbar = 1$ so that $\{B, J, \Delta, b\}$ are dimensionless parameters. In

the standard basis, $\mathcal{B} = \{ |00\rangle, |01\rangle, |10\rangle, |11\rangle \}$, the Hamiltonian (1) takes the following matrix form

$$H = \begin{pmatrix} \frac{1}{4}\Delta + B & 0 & 0 & 0 \\ 0 & -\frac{1}{4}\Delta - b & \frac{1}{2}J & 0 \\ 0 & \frac{1}{2}J & -\frac{1}{4}\Delta + b & 0 \\ 0 & 0 & 0 & \frac{1}{4}\Delta - B \end{pmatrix}. \tag{2}$$

By straightforward calculations, one can obtain the eigenvalues of Hamiltonian H as below

$$E_1 = \frac{1}{4}\Delta + B, \quad E_{2,3} = -\frac{1}{4}\Delta \pm \frac{1}{2}\chi, \quad E_4 = \frac{1}{4}\Delta - B, \tag{3}$$

with $\chi = \sqrt{J^2 + 4b^2}$. The corresponding eigenstates by means of the above standard basis are given as follows

$$|\psi_1\rangle = |00\rangle, \quad |\psi_{2,3}\rangle = \frac{1}{\sqrt{1+\eta_\pm^2}} (|10\rangle + \eta_\pm |01\rangle), \quad |\psi_4\rangle = |11\rangle, \tag{4}$$

where $\eta_\pm = \dfrac{J}{2b \pm \chi}$ is the inhomogeneity parameter [44].

2.2 Intrinsic decoherence

In general, any quantum system can be seen as an inevitably open system coupled to its surrounding environment. During the interaction with ancillary or interface systems, even a well-isolated system has to be at risk of losing its characteristic quantum traits, including coherence and quantum correlations. To describe this, Milburn amended the Schrödinger equation by incorporating a decay factor and presented a decoherence model, which is entirely of phase decoherence in the Markovian regime. According to Milburn's model [42], the time-dependent density matrix in the presence of intrinsic decoherence phenomenon is expressed as follows

$$\frac{\mathrm{d}}{\mathrm{d}t}\rho(t) = \frac{1}{\Gamma}[\exp(-i\Gamma H)\rho(t)\exp(i\Gamma H) - \rho(t)], \tag{5}$$

where Γ is the intrinsic decoherence parameter and H being the Hamiltonian of the system. It must be noticed that the master equation describing the intrinsic decoherence effect under Markovian approach writes as

$$\frac{\mathrm{d}}{\mathrm{d}t}\rho(t) = -i[H, \rho(t)] - \frac{\Gamma}{2}[H, [H, \rho(t)]]. \tag{6}$$

which can be derived from (5) for $\Gamma \longrightarrow 0$. Equation (6) corresponds to the standard von Neumann equation [45]. The formal solution of the master equation (6) can be written as

$$\rho(t) = \sum_{k=0}^{\infty} \frac{(\Gamma t)^k}{k!} M^k(t)\rho(0)(M^k(t))^\dagger, \tag{7}$$

where $\rho(0)$ being the initial state of the system and $M^k(t)$ is defined by

$$M^k(t) = H^k \exp(-iHt)\exp(-\Gamma H^2 t/2). \tag{8}$$

By inserting the complete relation $\sum_n ||\psi_n\rangle\rangle \langle\langle\psi_n|| = 1$ satisfied by the eigenvectors of the Hamiltonian (1) into Eq.(7), we obtain the following time-dependent density matrix

$$\rho(t) = \sum_{m,n} \exp\left(-\frac{\Gamma t}{2}(E_m - E_n)^2 - i(E_m - E_n)t\right) \times \langle\langle\psi_m|| \rho(0) ||\psi_n\rangle\rangle ||\psi_m\rangle\rangle \langle\langle\psi_n||. \tag{9}$$

Here, E_n and $||\psi_n\rangle\rangle$ denote the eigenvalues and eigenvectors of the Hamiltonian (1) given by Eq. (3) and (4), respectively.

2.3 Density operator

In this section, we shall examine the non-classical correlations by means of the so-called local quantum uncertainty and local Fisher information and entanglement measure in terms of concurrence inherent in a two-qubit system using the Heisenberg XXZ model in the presence of intrinsic decoherence phenomenon [42]. Indeed, let us assume that that the qubits are initially prepared in the extended Werner-like state as below [43]:

$$\rho(0) = r |\phi\rangle \langle\phi| + \frac{1-r}{4} I_4, \tag{10}$$

where r being the purity of the initial state $0 < r \leq 1$ while I is the (4×4) identity matrix and $|\phi\rangle$ is the well-known Bell-like state given by

$$|\phi\rangle = p\,|01\rangle + \sqrt{1 - p^2}\,|10\rangle, \tag{11}$$

with p is the degree of entanglement. In the standard basis, $\rho(0)$ can be written as

$$\rho(0) = \begin{pmatrix} \rho_{11}(0) & 0 & 0 & 0 \\ 0 & \rho_{22}(0) & \rho_{23}(0) & 0 \\ 0 & \rho_{23}(0) & \rho_{33}(0) & 0 \\ 0 & 0 & 0 & \rho_{44}(0) \end{pmatrix}, \tag{12}$$

where

$$\rho_{11}(0) = \rho_{44}(0) = \frac{1-r}{4}, \quad \rho_{22}(0) = rp^2 + \frac{1-r}{4}, \quad \rho_{33}(0) = r(1-p^2) + \frac{1-r}{4}, \rho_{23}(0) = rp\sqrt{1-p^2}. \tag{13}$$

From the equation (9), the time evolution of the density matrix can be written as

$$\rho(t) = \begin{pmatrix} \rho_{11}(t) & 0 & 0 & 0 \\ 0 & \rho_{22}(t) & \rho_{23}(t) & 0 \\ 0 & \rho_{*23}(t) & \rho_{33}(t) & 0 \\ 0 & 0 & 0 & \rho_{44}(t) \end{pmatrix}. \tag{14}$$

where the density matrix elements are given by

$$\rho_{11}(t) = \rho_{11}(0) = \frac{1-r}{4},$$

$$\rho_{22}(t) = \frac{1}{2\chi^2}((8b^2 + J^2)\rho_{22}(0) + 4bJ\rho_{23}(0) + J^2\rho_{33}(0) + J\exp(-\tfrac{1}{2}\chi^2 t\Gamma)(J\rho_{22}(0) - 4b\rho_{23}(0) - J\rho_{33}(0))\cos(\chi t)),$$

$$\rho_{33}(t) = \frac{1}{2\chi^2}(J^2\rho_{22}(0) - 4bJ\rho_{23}(0) + (8b^2 + J^2)\rho_{33}(0) + J\exp(-\tfrac{1}{2}\chi^2 t\Gamma)(-J\rho_{22}(0) + 4b\rho_{23}(0) + J\rho_{33}(0))\cos(\chi t)),$$

$$\rho_{23}(t) = \frac{1}{2\chi^2}\begin{pmatrix} 2J\exp(\tfrac{1}{2}\chi^2 t\Gamma)(b\rho_{22}(0) + J\rho_{23}(0) - b\rho_{33}(0)) + 2b(-J\rho_{22}(0) + 4b\rho_{23}(0) \\ + J\rho_{33}(0))\cos(\chi t) + i\chi(J\rho_{22}(0) - 4b\rho_{23}(0) - J\rho_{33}(0))\sin(\chi t) \end{pmatrix}\exp(-\tfrac{1}{2}\chi^2 t\Gamma),$$

$$\rho_{44}(t) = \rho_{44}(0) = \frac{1-r}{4}. \tag{15}$$

Note that $\rho_{11}(t)$ and $\rho_{44}(t)$ are not affected by the decoherence phenomenon since $\rho_{11}(t) = \rho_{11}(0)$ and $\rho_{44}(t) = \rho_{44}(0)$. Moreover, the eigenvalues of the density matrix in Eq.(14) are calculated as below:

$$\lambda_1 = \lambda_2 = \rho_{11}(t),$$

$$\lambda_3 = \frac{1}{2}[\rho_{22}(t) + \rho_{33}(t) - \sqrt{(\rho_{22}(t) - \rho_{33}(t))^2 + 4|\rho_{23}(t)|^2}],$$

$$\lambda_4 = \frac{1}{2}[\rho_{22}(t) + \rho_{33}(t) + \sqrt{(\rho_{22}(t) - \rho_{33}(t))^2 + 4|\rho_{23}(t)|^2}], \tag{16}$$

while the corresponding eigenvectors turn out to be:

$$|\lambda_1\rangle = |11\rangle,$$

$$|\lambda_2\rangle = |00\rangle,$$

$$|\lambda_3\rangle = \frac{1}{\sqrt{1 + |\omega|^2}}(\omega\,|01\rangle + |10\rangle),$$

$$|\lambda_4\rangle = \frac{1}{\sqrt{1 + |\varkappa|^2}}(\varkappa\,|01\rangle + |10\rangle), \tag{17}$$

where

$$\omega = \frac{1}{2\rho_{*23}(t)}[\rho_{22}(t) - \rho_{32}(t) - \sqrt{(\rho_{22}(t) - \rho_{33}(t))^2 + 4|\rho_{23}(t)|^2}],$$

$$\varkappa = \frac{1}{2\rho_{*23}(t)}[\rho_{22}(t) - \rho_{32}(t) + \sqrt{(\rho_{22}(t) - \rho_{33}(t))^2 + 4|\rho_{23}(t)|^2}]. \tag{18}$$

3 Quantum correlations

We begin in this section by introducing some non-classical correlations quantifiers, namely LQU and LQFI and the concurrence.

3.1 Quantum entanglement: concurrence

Various measures have been proposed to quantify the amount of entanglement in bipartite and multipartite quantum systems. The concurrence $\mathcal{C}$ introduced by W.K. Wootters has been proven to be particularly useful and it is the most popular computable measure for arbitrary two-qubit mixed states. This simple approach was developed to distinguish quantum entangled states from separable states qualitatively and quantitatively. Indeed the case reflects $\mathcal{C} = 0$ happens when the system is unentangled (separable), whereas $\mathcal{C} = 1$ reveals a maximally entangled state. The concurrence is given by [17]

$$\mathcal{C} = \max\{0, \sqrt{\delta_1} - \sqrt{\delta_2} - \sqrt{\delta_3} - \sqrt{\delta_4}\}, \tag{19}$$

where $\delta_i (i = 1, 2, 3, 4)$ are the eigenvalues in the decreasing order of the 4×4 matrix $R = \rho(\sigma^y \otimes \sigma^y)\rho^*(\sigma^y \otimes \sigma^y)$, in which ρ^* and σ^y are, respectively, the complex conjugate of ρ in the standard basis and the $y-$component Pauli matrix. For the density matrix (14), the concurrence is given by

$$\mathcal{C}(\rho(t)) = 2 \max\{0, |\rho_{23}(t)| - \sqrt{\rho_{11}(t)\rho_{44}(t)}\}. \tag{20}$$

The concurrence of the initial state $\rho(0)$ (10) can be derived from (20). It writes as

$$\mathcal{C}(\rho(0)) = 2 \max\{0, r(p\sqrt{1 - p^2} + \frac{1}{4}) - \frac{1}{4}\}. \tag{21}$$

Hence, the initial state $\rho(0)$ (10) is entangled when $r > r_0 = 1/(1 + 4p\sqrt{1 - p^2})$. However, for $r \leq r_0$, the concurrence (21) is zero and the entanglement vanishes and the initial state $\rho(0)$ (10) becomes separable. For example, when the state of Eq.(11) becomes the Bell state for the value $p = \frac{1}{\sqrt{2}}$, then, in this case $\rho(0)$ is simply the Werner-like state. It is entangled when $r > \frac{1}{3}$.

3.2 Local quantum uncertainty

Due to the probabilistic character of quantum mechanics, two incompatible observables cannot be measured simultaneously with arbitrary precision. The uncertainty principle imposes a fundamental bound on the precision. The total uncertainty due to a single observable K measurement on a quantum state ρ is usually defined by the following variance

$$\text{Var}(\rho, K) = \text{Tr}(\rho K^2) - (\text{Tr}(\rho K))^2. \tag{22}$$

This uncertainty has purely quantum nature for pure states. However, it may include both classical ignorance due to the state mixedness and genuinely quantum part arising by the non-commutativity of a state with an acting observable. In the theory of quantum information, it is essential to distinguish between classical and quantum components. In order to deal only with quantum part of the variance, Wigner and Yanase introduced the notion of the so-called skew information as a good quantifier of this uncertainty [20]. It is defined as follows

$$\mathcal{I}(\rho, K) = -\frac{1}{2}\text{Tr}([\sqrt{\rho}, K]^2), \tag{23}$$

where $[.,.]$ is the commutator, while $\mathcal{I}$ is the skew information associated to the density matrix ρ. It is worth nothing that, unlike variance, Wigner–Yanase skew information (WYSI) is unaffected by classical mixing and it reduces to the variance for pure states. Based on the notion of skew information, a discord-like measure of quantum correlations was recently proposed by Girolami et al for arbitrary bipartite quantum systems [18]. This measure called local quantum uncertainty and defined as the minimum skew information achievable with a single local measurement. It is given by

$$\mathcal{U}_A(\rho) = \min_{K_A} \mathcal{I}(\rho, K_A \otimes I_B), \tag{24}$$

where K_A is a Hermitian operator (local observable) on the subsystem A admitting a non-degenerate spectrum. Moreover, I_B being the identity operator acting on the subsystem B. Note that, $\mathcal{I}$ is non-negative and non-increasing under classical mixing [19]. Besides, LQU quantifies the minimum amount of uncertainty in a quantum state and is inherently an asymmetric quantity with respect to subsystem exchange because they depend on which subsystem the measurements are made on [18,21]. From now on, we consider the simple form $\mathcal{U}(\rho)$ instead of $\mathcal{U}_A(\rho)$. For a $2 \otimes d$ (qubit–qudit) bipartite quantum systems [18], the closed-form of the local quantum uncertainty turns out to be,

$$\mathcal{U}(\rho) = 1 - \max(\zeta_1, \zeta_2, \zeta_3), \tag{25}$$

where $\zeta_i (i = 1, 2, 3)$ are the eigenvalue of the 3×3 matrix $\mathcal{W}$ of the following elements:

$$(\mathcal{W})_{\alpha\beta} = \text{Tr}(\sqrt{\rho} \left(\sigma^\alpha \otimes I_B\right) \sqrt{\rho} \left(\sigma^\beta \otimes I_B\right)), \tag{26}$$

where $\sigma^\alpha(\sigma^\beta)$ with $\alpha(\beta) = \{x, y, z\}$ represent the Pauli operators of the subsystem A. The local quantum uncertainty provides a reliable quantifier of quantum correlations and it has a geometrical significance in terms of Hellinger distance [18]. It is clear that having the matrix $\mathcal{W}$, one can easily evaluate the local quantum uncertainty for qubit–qudit quantum systems contrarily to quantum discord based on von Neumann entropy [19,46]. This is a quite an easy task compared with the complicated minimization process over parameters due to the local measurements [18,29]. It is important to note that for some quantum states, quantum discord and local quantum uncertainty capture the same correlations, whereas, they are different measures for others states [19]. However, for the pure bipartite states, the local quantum uncertainty reduces to the linear entropy of the reduced densities of the subsystems and vanishes for classically correlated state [18]. Moreover, it is invariant under local unitary operations [18].

In the Fano–Bloch representation, the density matrix $\rho(t)$ (14) can be written as follows:

$$\rho(t) = \frac{1}{4} \sum_{\mu,\nu=0}^{3} \mathcal{R}_{\mu\nu}(t) \left(\sigma^\mu \otimes \sigma^\nu\right), \tag{27}$$

where $\mathcal{R}_{\mu\nu}(t) = \text{Tr}\left(\rho(t)(\sigma^\mu \otimes \sigma^\nu)\right)$ are the total correlation tensor components occurring in the Fano–Bloch decomposition associated with bipartite density matrix $\rho(t)$ with $\sigma^\mu(\sigma^\nu) = \{\sigma^0, \sigma^\alpha(\sigma^\beta)\}$. The non-vanishing components $\mathcal{R}_{\mu\nu}(t)$ are calculated as

$$\mathcal{R}_{00}(t) = \text{Tr}\rho(t) = 1, \quad \mathcal{R}_{03}(t) = 1 - 2(\rho_{22}(t) + \rho_{44}(t)), \quad \mathcal{R}_{11}(t) = \mathcal{R}_{22}(t) = |\rho_{23}(t)|,$$
$$\mathcal{R}_{30}(t) = 1 - 2(\rho_{33}(t) + \rho_{44}(t)), \quad \mathcal{R}_{33}(t) = 1 - 2(\rho_{22}(t) + \rho_{33}(t)). \tag{28}$$

Therefore, in terms of the Fano–Bloch components $\mathcal{R}_{\mu\nu}(t)$ associated with the matrix $\rho(t)$ (14), the eigenvalues of the 3×3 matrix $(\mathcal{W}(t))_{\alpha\beta}$ (26) can be expressed as

$$\mathcal{W}_{11}(t) = \mathcal{W}_{22}(t) = \sqrt{\left(t_1(t) + 2\sqrt{d_1(t)}\right)\left(t_2(t) + 2\sqrt{d_2(t)}\right)} + \frac{1}{4} \frac{\left(\mathcal{R}_{03}^2(t) - \mathcal{R}_{30}^2(t)\right)}{\sqrt{\left(t_1(t) + 2\sqrt{d_1(t)}\right)\left(t_2(t) + 2\sqrt{d_2(t)}\right)}}, \tag{29}$$

$$\mathcal{W}_{33}(t) = \frac{1}{2}\left(1 + 2\left(\sqrt{d_1(t)} + \sqrt{d_2(t)}\right)\right)$$
$$+ \frac{1}{8}\left(\frac{(\mathcal{R}_{03}(t) + \mathcal{R}_{30}(t))^2 - (\mathcal{R}_{11}(t) - \mathcal{R}_{22}(t))^2}{\left(t_1(t) + 2\sqrt{d_1(t)}\right)} + \frac{(\mathcal{R}_{03}(t) - \mathcal{R}_{30}(t))^2 - (\mathcal{R}_{11}(t) + \mathcal{R}_{22}(t))^2}{\left(t_2(t) + 2\sqrt{d_2(t)}\right)}\right), \tag{30}$$

where

$$t_{1,2}(t) = \frac{1}{2}\left(\mathcal{R}_{00}(t) \pm \mathcal{R}_{03}(t)\right), \tag{31}$$

$$d_{1,2}(t) = \frac{1}{16}\left[(\mathcal{R}_{00}(t) \pm \mathcal{R}_{33}(t))^2 - (\mathcal{R}_{30}(t) \pm \mathcal{R}_{03}(t))^2 - (\mathcal{R}_{11}(t) \mp \mathcal{R}_{22}(t))^2\right].$$

Hence, in this case, it is easy to check that the matrix $(\mathcal{W}(t))_{\alpha\beta}$ (26) is diagonal $(\mathcal{W}_{12}(t) = \mathcal{W}_{21}(t) = \mathcal{W}_{23}(t) = \mathcal{W}_{32}(t) = \mathcal{W}_{13}(t) = \mathcal{W}_{31}(t) = 0)$. Thus, its eigenvalues are simply reduced to diagonal elements $\mathcal{W}_{ii}(t)$ $(i = 1, 2, 3)$. Therefore, the LQU associated with quantum correlation in the system described by $\rho(t)$ (14) takes the form

$$\mathcal{U}(\rho(t)) = 1 - \max(\mathcal{W}_{11}(t), \mathcal{W}_{22}(t), \mathcal{W}_{33}(t)). \tag{32}$$

3.3 Local quantum Fisher information

Quantum Fisher Information has been shown to be an useful concept in quantum estimation theory. It is employed to determine the precision of a parameter associated with a physical quantity encoded in the quantum state. Assume that ρ_ϵ is an arbitrary quantum state, where ϵ is the parameter to be estimated, the QFI is defined as follows [47,48]

$$F(\rho) = \frac{1}{4}\text{Tr}[\rho_\epsilon \mathcal{L}_\epsilon^2], \tag{33}$$

where $\mathcal{L}_\epsilon$ denotes the symmetric logarithmic derivative operator that satisfies the following equation :

$$\frac{\partial \rho_\epsilon}{\partial \epsilon} = \frac{1}{2}(\mathcal{L}_\epsilon \rho_\epsilon + \rho_\epsilon \mathcal{L}_\epsilon). \tag{34}$$

Now, suppose that the initial density operator, namely $\rho(0)$ evolves unitarily and the corresponding unitary operation is $\mathcal{U}_\epsilon = e^{iH\epsilon}$ such as $\rho_\epsilon = \mathcal{U}_\epsilon^\dagger \rho(0)\mathcal{U}_\epsilon$. In this case, the QFI can be expressed in terms of the Hamiltonian H (1) governing the evolution of the system [49]

$$F(\rho, H) = \frac{1}{2} \sum_{i \neq j} \frac{(\lambda_i - \lambda_j)^2}{\lambda_i + \lambda_j} |\langle \lambda_i | H | \lambda_j \rangle|^2, \tag{35}$$

where $\rho = \sum_n \lambda_n |\lambda_n\rangle\langle\lambda_n|$. It follows when the dynamics is governed by a local transformation, namely $e^{-i\epsilon H_A}$ of a local Hamiltonian $H_A = H_a \otimes I_B$, the so-called local quantum Fisher information turns out to be:

$$F(\rho, H_A) = \mathrm{Tr}[\rho H_A^2] - \sum_{i \neq j} \frac{2\lambda_i \lambda_j}{\lambda_i + \lambda_j} |\langle \lambda_i | H_A | \lambda_j \rangle|^2. \tag{36}$$

The main motivation behind the use LQFI is its ability to serve as good witness of quantum correlations. The quantum quantum correlations measured by means of LQFI correspond to the minimum of QFI over all local Hamiltonians H_A acting on the part A [50]. It is given by

$$Q(\rho(t)) = \min_{H_A} F(\rho, H_A). \tag{37}$$

We notice that the local Hamiltonian can be expressed in terms of the Pauli matrices, namely σ^α and Bloch vector r^α ($\alpha = x, y, z$) as $H_A = \sigma^\alpha . r^\alpha$, such that $|r^\alpha| = 1$ [50]. It follows that the first term on the right-hand side of Eq.(36) is equal to one, while the second term leads to:

$$\begin{aligned}
\sum_{i \neq j} \frac{2\lambda_i \lambda_j}{\lambda_i + \lambda_j} |\langle \lambda_i | H_A | \lambda_j \rangle|^2 &= \sum_{i \neq j} \frac{2\lambda_i \lambda_j}{\lambda_i + \lambda_j} |\langle \lambda_i | H_A | \lambda_j \rangle\langle \lambda_j | H_A | \lambda_i \rangle \\
&= \sum_{i \neq j} \sum_{\alpha=\beta=1}^{3} \frac{2\lambda_i \lambda_j}{\lambda_i + \lambda_j} \langle \lambda_i | (r^\alpha \sigma^\alpha) \otimes I_B | \lambda_j \rangle\langle \lambda_j | (r^\beta \sigma^\beta) \otimes I_B | \lambda_i \rangle \\
&= r^\alpha \sum_{i \neq j} \sum_{\alpha=\beta=1}^{3} \frac{2\lambda_i \lambda_j}{\lambda_i + \lambda_j} \langle \lambda_i | \sigma^\alpha \otimes I_B | \lambda_j \rangle\langle \lambda_j | \sigma^\beta \otimes I_B | \lambda_i \rangle r^\beta \\
&= r^\alpha S_{\alpha\beta} r^\beta \\
&= r^T . S . r
\end{aligned} \tag{38}$$

where $\sigma^1 \equiv \sigma^x$, $\sigma^2 \equiv \sigma^y$ and $\sigma^3 \equiv \sigma^z$. Moreover, S denotes a 3×3 symmetric matrix with the following elements

$$(S)_{\alpha\beta} = \sum_{m \neq n} \frac{2\lambda_m \lambda_n}{\lambda_m + \lambda_n} \langle \lambda_m | \sigma^\alpha \otimes I_B | \lambda_n \rangle\langle \lambda_n | \sigma^\beta \otimes I_B | \lambda_m \rangle. \tag{39}$$

The minimum over all unit of vectors r^α which coincide with the maximum eigenvalues of S and the LQFI is obtained as [50]

$$Q(\rho(t)) = 1 - \lambda_{\max}^S. \tag{40}$$

This quantity is invariant under any local unitary operation, non-negative and vanishes for any kind of classically correlated states. Moreover, it coincides the geometric discord for pure quantum states [50]. After some straightforward calculations and using the eigenvalues and eigenvectors calculated in Eqs. (16) and (17), the analytical expression of LQFI is obtained as

$$Q(\rho(t)) = 1 - \max(S_{11}, S_{22}, S_{33}), \tag{41}$$

where $S_{\alpha\alpha}$ ($\alpha = 1, 2, 3$) are calculated analytically from Eq. (39). They are given by

$$\begin{aligned}
S_{11} = S_{22} &= 4\frac{\lambda_1 \lambda_3}{\lambda_1 + \lambda_3} |\omega|^2 + 4\frac{\lambda_1 \lambda_4}{\lambda_1 + \lambda_4} |\varkappa|^2 + 4\frac{\lambda_2 \lambda_3}{\lambda_2 + \lambda_3} + \frac{\lambda_2 \lambda_4}{\lambda_2 + \lambda_4} |\omega|^2, \\
S_{33} &= 4\frac{\lambda_3 \lambda_4}{\lambda_3 + \lambda_4} |\omega^* \varkappa - 1|^2.
\end{aligned} \tag{42}$$

where λ_i ($i = 1, \ldots, 4$), ω and $\varkappa$ are given in Eqs. (16) and (18), respectively. Moreover, we have $S_{12} = S_{21} = S_{23} = S_{32} = S_{13} = S_{31} = 0$. Interestingly enough, one of the most important properties of LQU in relation with LQFI is: given any unitary evolution, the LQU is majorized by LQFI as follows [22,23]

$$\mathcal{U}(\rho(t)) \leq \mathcal{I}(\rho(t), H) \leq Q(\rho(t)), \tag{43}$$

where $\mathcal{U}(\rho(t))$ and $Q(\rho(t))$ are the LQU and LQFI defined in Eqs.(25) and (40), respectively. Moreover, $\mathcal{I}(\rho(t), H)$ denotes the skew information defined in Eq.(23).
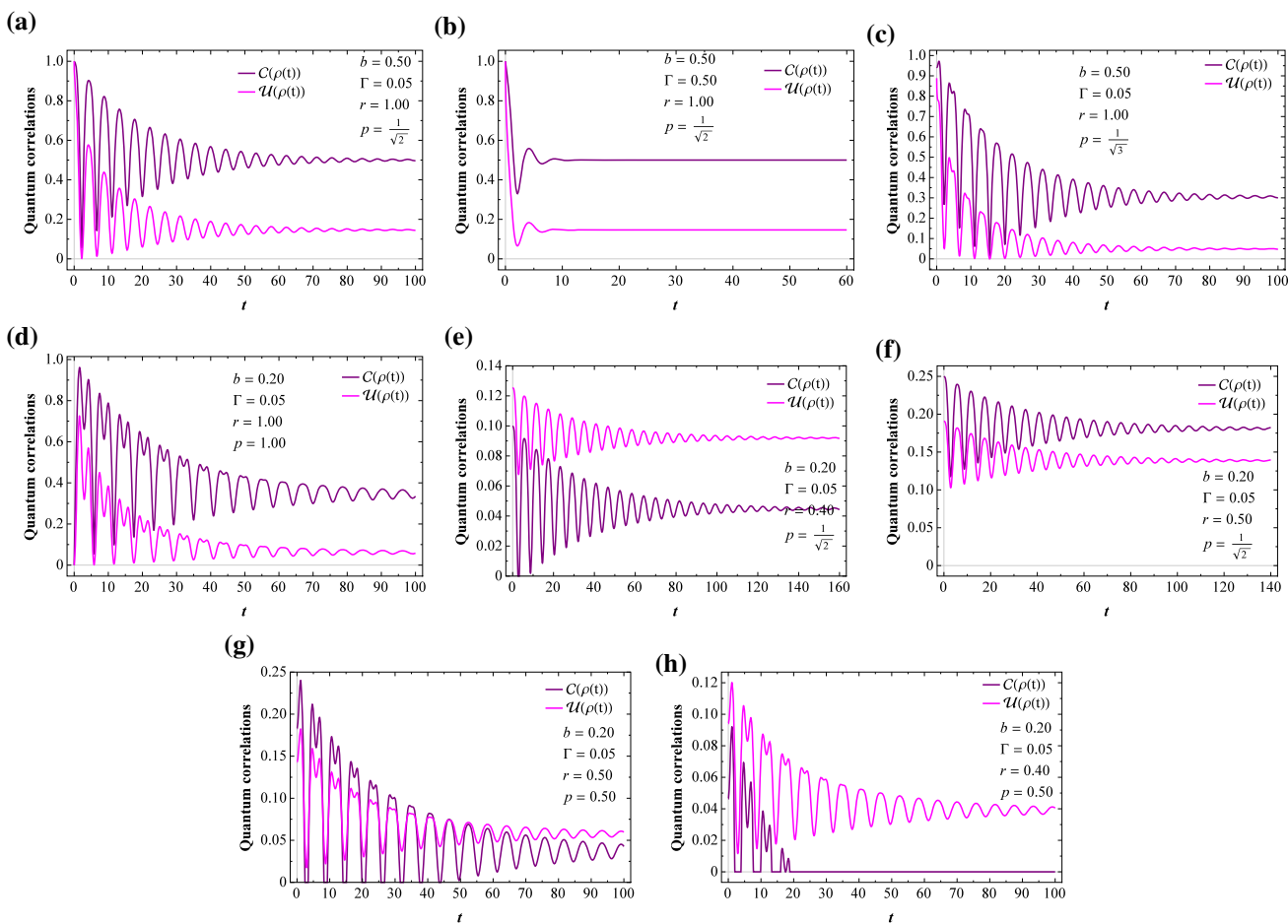
Fig. 1 Dynamics of quantum correlations versus time parameter t for several fixed values of purity parameter p and degree of entanglement r, assuming fixed $J = 1$

4 Analysis of quantum correlations evolution

To get an insight into the dynamics of the bipartite quantum correlations for the model under intrinsic decoherence, we have plotted in Fig. 1 the temporal evolution of the concurrence $\mathcal{C}$ and local quantum uncertainty (LQU) for several values of the purity r and the entanglement degree parameter p and we considered the following value of $J = 1$. Figure 1a, b depicts the behaviors when $r = 1$ and $p = 1/\sqrt{2}$ corresponding to the case where the system is initially prepared in the maximally entangled pure state; $|\phi\rangle = \frac{1}{\sqrt{2}}(|01\rangle + |10\rangle)$. In this case, for $t = 0$, both measures $\mathcal{C}$ and LQU are maximal $\mathcal{C} = 1$ and $\mathcal{U} = 1$, which means that two-qubit are maximally entangled. Moreover, both quantum correlations quantifiers decrease during the decoherence process. When $\Gamma = 0.05$ (Fig. 1a), the LQU shows a set of damping oscillations with series of revival and collapse phenomena over time with an asymptotic limit. All measures reach a steady-state value, which means that the amount of quantum correlation is frozen for specific intervals of time. Note that the time variations for the concurrence $\mathcal{C}$ show large amplitudes compared to those displayed for LQU. Figure 1b shows also that large numbers of the intrinsic decoherence rate ($\Gamma = 0.50$) accelerate the stabilization of correlations at the same steady-state values. Further, the two-qubit state exhibits frozen dynamics for both measures. On the other hand, the oscillatory behavior of parameters is almost disappeared due to the intrinsic decoherence effect. The increment of the decoherence intrinsic rate Γ causes fast correlations measures decay and shows that the intrinsic decoherence plays a destructive effect on the quantum correlations. As we mentioned, the steady-state value does not depend on Γ, but it depends on the system's initial state.

Figure 1c shows the evolution of parameters $\mathcal{C}$ and LQU when the system is initially in a pure Bell-shaped state ($r = 1$) with $p = 1/\sqrt{3}$. This case corresponds to the state $\rho(0) = |\phi\rangle\langle\phi|$ with $|\phi\rangle = \frac{1}{\sqrt{3}}(|01\rangle + \sqrt{2}|10\rangle)$. Figure 1c shows that the LQU reaches its maximum value at $t = 0$, whereas the concurrence has a minimum value at which the time parameter t is close to absolute zero. Besides, we can also see that the concurrence has a sharp maximum positioned around $t \approx 1$. However, the maximum bound of the concurrence is higher than LQU. When the dynamic is switched on, both quantifiers decrease following the same behaviors as plotted in Fig. 1a, b but with many oscillations frequencies of the amount of quantum correlations between the two-qubit. It is clear, the robust value of the amplitude of those functions asymptotically decreases. Moreover, the frozen phenomenon appears also in
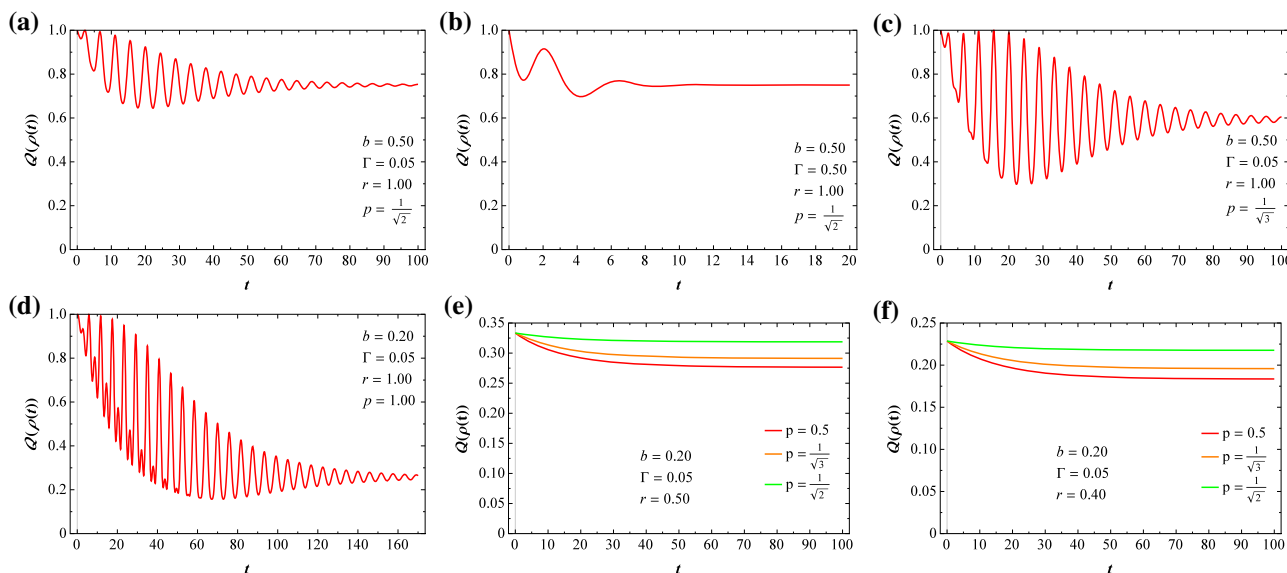
Fig. 2 Dynamics of local Fisher information versus the time parameter t for several fixed values of purity parameter p and degree of entanglement r, assuming fixed $J = 1$

this pure state. Figure 1d shows the evolution of $\mathcal{C}$ and LQU versus the time, when the system is initially separable $p = 1$ (i.e., $\rho(0) = |01\rangle\langle01|$), at $t = 0$ there are no quantum correlations between the qubits. However, with time increasing, the quantum correlations between two spin-1/2 qubits can be generated by the time evolution of the state under the Hamiltonian (1), implying that the spin–spin interaction is responsible for the induced correlation between the qubits by a series of entanglement revival and collapse phenomena. This conclusion is also similar to the results reported in Ref. [51] where the generation of non-classical correlations is due to the coupling parameter between an atomic system interacting with a single mode of radiation field inside a quantum electrodynamics cavity, in such a way large numbers of the coupling parameter allow in general to increase gradually quantum correlations. Further, the dynamics of concurrence differ from the LQU. The amplitudes of the concurrence $\mathcal{C}$ are always larger than those obtained for LQU. Moreover, the LQU stabilizes for a particular time interval, which means that the LQU is frozen. The LQU correlations are more stable than the concurrence (the LQU stabilizes at a steady-state value lower than the concurrence). By fixing the degree of entanglement at the value $p = 1/\sqrt{2}$, the state (10) turns out to be the Werner state. From equation (21), one can see that when the purity r is ranging between 0.3 and 1, the system is initially entangled, otherwise it is disentangled. We notice that even if the system is separable ($\mathcal{C} = 0$ for $0 \leq r \leq 1/3$), the LQU remains nonzero. It implies that quantum entanglement is only a special kind of quantum correlation and even separable states possess the quantum correlations.

Figure 1e, f shows the time evolution of the concurrence and LQU for $r = 0.4$ and $r = 0.5$, respectively, when the Werner state is considered as the initial state. Figure 1e, f indicates that the LQU takes a maximum bound comparing to the concurrence when $r = 0.4$, but when the purity switches to $r = 0.5$ the concurrence is larger than the LQU. At $t = 0$, both qubits are partially entangled. When the dynamics is switched on the quantum correlations decrease until reaching a constant value. From Fig. 1e, it is clear that the concurrence vanishes instantly for particular time values. For these particular values, the disentangled two qubits have non-zero LQU. The amplitudes of the parameter $\mathcal{C}$ are always larger than those displayed for the LQU, even if the LQU predominates over $\mathcal{C}$. By comparing the results of Fig. 1f with Fig. 1e, we can conclude that the increase of the purity r leads to the correlations enhancement as well as their robustness against the decoherence. The oscillations frequencies become more prominent for the two-qubit system as the purity strength r decreases. The time evolution of the concurrence and LQU, when the system is initially prepared in the mixed state, are shown in Fig. 1g, h, respectively, in the case when $r = 0.4$ and $r = 0.5$. They show different behaviors compared to those shown for concurrence and LQU in the previous cases. For the initially mixed state, we observed that the dynamics under intrinsic decoherence cause entanglement sudden death, while LQU quantity is more robust than entanglement. This indicates that there exists locality by means of LQU even in the absence of entanglement between the subsystems. The amplitudes of the concurrence are always larger than those of the LQU. The phenomena of sudden death and growth of entanglement appear in the behavior of the concurrence entanglement, where the two qubits have a non-zero LQU correlation. Both quantifiers reach a steady-state demonstrating the frozen phenomenon. Interestingly, when the purity switches to $r = 0.4$, the entanglement oscillates at a particular time interval and after some time the entanglement between the qubits remains zero and it is known as the sudden death of entanglement. On the other hand, the LQU keeps the same behavior as plotted in Fig. 1g. Thus, from Fig. 1, we conclude that the LQU correlation is more stable than the concurrence. The stability of the generated correlations is enhanced. The frozen LQU and $\mathcal{C}$ show a robust feature against the intrinsic decoherence.
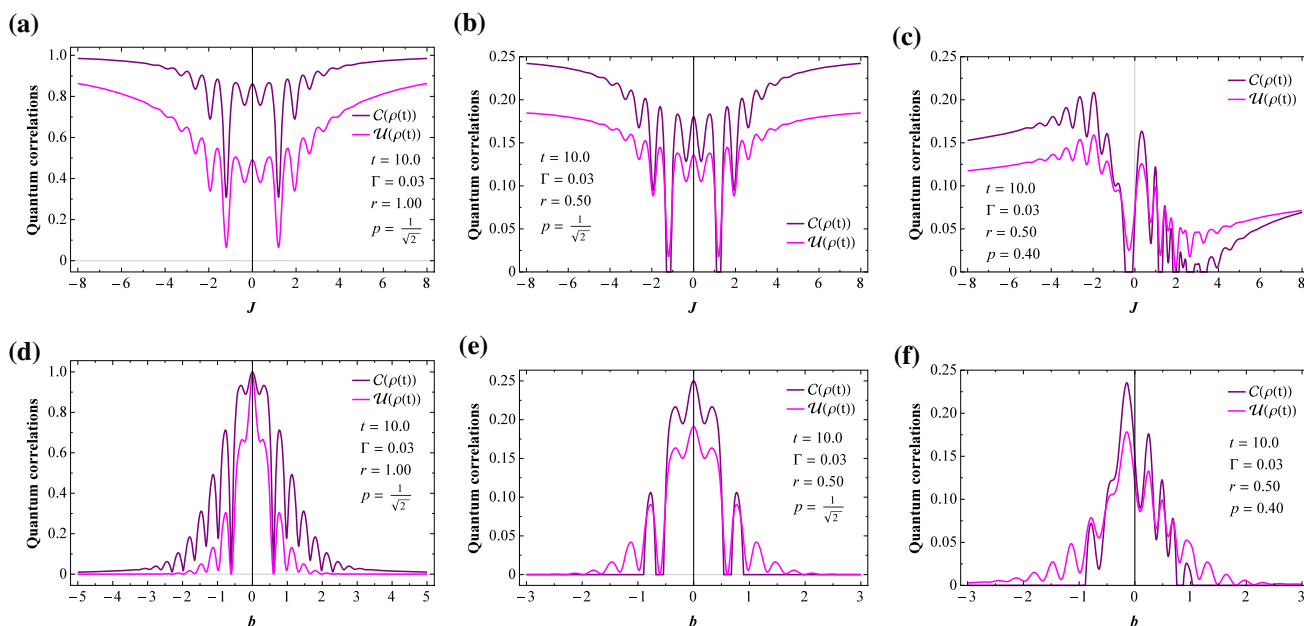
Fig. 3 Upper panels: dynamics of quantum correlations as a function of the exchange coupling parameter J when the system is initially prepared in the maximally entangled state (**a**), in the Werner state (**b**), and in the mixed state (**c**), taking $b = 0.20$, $t = 10$ and $\Gamma = 0.03$. Lower panels: dynamics of quantum correlations as a function of the inhomogeneous magnetic field b when the system is initially prepared in the maximally entangled state (**d**), in the Werner state (**e**), and in the mixed state (**f**), taking $J = 1$, $t = 10$ and $\Gamma = 0.03$

Figure 2 displays the dynamical evolution of LQFI versus the time t for different initial settings of b, r, p and Γ. In the case when $r = 1$ and $p = \frac{1}{\sqrt{2}}$, corresponding to a maximally entangled state, the state $\rho(t)$ defined in Eq.(14) is initially maximally entangled state since the LQFI reaches its maximum for $t = 0$. Under decoherence effects, the LQFI decreases gradually to stabilize for a specific interval of time which means that the LQFI becomes frozen. Moreover, it is clear that for small values of decoherence parameter Γ (Fig. 2a) gives oscillating variation of quantum correlations similar to those displayed for higher values of Γ (See Fig. 2b) which allows to enhance the stability of quantum correlations by means of LQFI. On the other hand, it is clear that even in the presence of decoherence phenomenon, the sudden death phenomenon does not occur. In Fig. 2c, d, we analyze the LQFI quantifier for a pure state, namely $r = 1$ and $p \neq \frac{1}{\sqrt{2}}$. As it can be seen, the LQFI follows the same behaviors as in Fig. 2a, b but with many oscillations frequencies of the quantum correlations between the two-qubit system. Again, it is clear that the presence of decoherence phenomenon doesn't possess the sudden death phenomenon but leads to froze the LQFI for large values of t. However, Fig. 2e, f shows the evolution of non-classical correlations by means of LQFI for different values of p. Indeed, for $p = \frac{1}{\sqrt{2}}$, the state is simply the Werner state. In this case, it is clear that both the oscillation correlations and the sudden death phenomena don't occur while the frozen phenomenon appears fast. The entanglement sudden death does not necessarily mean the loss of all quantum correlations. As separate states nevertheless have an advantage over classical states, thus they are still relevant for protocols that exploit quantum correlations other than entanglement. However, an efficient information processing protocol based on the local quantum Fisher information offers more resistance to the effect of intrinsic decoherence and is completely different from that of entanglement.

From Figs. 1 and 2, it is clear that in most of the above-cited cases, the non-classical correlations quantified by means of LQFI and LQU and the entanglement measure in terms of concurrence follow the same behavior but different upper bounds and various oscillations correlations. Moreover, it is obvious that the sudden death and the sudden growth phenomena appear in the LQU and concurrence behaviors while they don't occur for LQFI. On the other hand, the amplitudes of LQFI are always robust than those displayed for LQU and concurrence. The results discussed above show that the local quantum Fisher information is always greater than the LQU and the concurrence. This agrees with the results given by the inequality (40).

An interesting topic is to investigate an overall insight into the influence of the inhomogeneous magnetic field and the coupling coefficients, namely b and J, respectively, on the dynamics of concurrence and local quantum uncertainty. Indeed, in Fig. 3a–c and Fig. 3e–g, we investigate the evolution of the $\mathcal{C}$ and LQU for the system which is initially prepared in the maximally entangled state, in the Werner state, and in the mixed state as a function of parameters and J, respectively. The time and the intrinsic rate have been fixed at $t = 10$ and $\Gamma = 0.03$. When the system is initially prepared in the maximally entangled state, it is clear from Fig. 3a that the concurrence and LQU are symmetric with respect to $J = 0$. As $|J|$ increases, both quantifiers show oscillations until reaching a maximal asymptotic constant value. This shows that the coupling J enhances the amount of quantum correlations in the system. We notice that both measures have similar behavior but with different amplitudes; therefore, they can give the same information about

the correlations of the qubits and they present a freezing phenomenon for higher values of $|J|$ (the amount of quantum correlations is constant).

From Fig. 3a, it is quite clear that the concurrence is more robust than LQU when the initial states of qubits are maximally entangled. For the case of the Werner state Fig. 3b when $r = 0.5$ and $p = 1/\sqrt{2}$, the entanglement quantified by the concurrence and LQU have similar behavior as shown in Fig. 3a. For particular values of J ($|J| = 1.5$), the concurrence exhibits the phenomena of sudden death and growth entanglement, while the two qubits have non-zero LQU. The concurrence and LQU present an unusual behavior (see Fig. 3c) when the system is initially prepared in the mixed state. First, both measures are not symmetric with respect to $J = 0$. Both quantifiers have more oscillations frequencies in the antiferromagnetic phase ($J > 0$). The concurrence shows the death and growth phenomena with an increase of coupling constant until it reaches a steady state, while the LQU decreases gradually with a tendency of stabilization. Note that the maximum values achieved by LQU are larger than those displayed for entanglement. In the ferromagnetic phase ($J < 0$), for a particular point, $\mathcal{C}$ shows the death and growth phenomenon and then continues to oscillate until it stabilizes. The asymptotic value reached for the antiferromagnetic phase ($J > 0$) is higher than one evaluated for the ferromagnetic phase ($J < 0$). This is due to the ground-state phase transition in the Heisenberg XXZ spin chain H (1) [3,29]. As a result, the quantum correlations in the ferromagnetic phase are most robust than those given in the anti-ferromagnetic phase, when the system is initially prepared in the mixed state. The ferromagnetic property enhances the quantum correlations in the two-qubit system. On the other hand, introducing J into a constructive domain could generate and improve the quantum correlations in the system. This result can be understood as follows: the information between two spin-1/2 qubits is controlled by different parameters in Heisenberg spin chain systems. Some proportionally while some negatively affect the information as well as other correlations between them. One of the parameters, regulating the exchange coupling, directly increases the information transfer rate between the two qubits. Thus, the two qubits become more entangled and correlated as the exchange coupling parameter strength increase and vice versa.

Figure 3d presents the effect of the inhomogeneous magnetic field on the concurrence and LQU for $r = 1$ and $p = 1/\sqrt{2}$. It is clear that the $\mathcal{C}$ and LQU reach their maximum ($\mathcal{C} = 1$ and $\mathcal{U} = 1$) for $b = 0$ and the qubits are maximally correlated. Both quantifiers exhibit sudden revival and collapse phenomena which manifests themselves in increasingly weak peaks as $|b|$ increases. LQU collapses faster than $\mathcal{C}$, which decreases very slowly. This indicates that the LQU is more sensitive to the inhomogeneous magnetic field than $\mathcal{C}$ when the system is prepared in the maximally entangled state. When the system is prepared in the Werner state (Fig. 3e), the concurrence and LQU have nearly the same behavior as plotted in Fig. 3d, except that the concurrence collapses fast for a small period of time which indicates the phenomenon of entanglement sudden death (ESD). This surprising behavior was reported in [52]. The LQU keeps a non-zero value, decreases with oscillations, and becomes zero with an increase of $|b|$, but without any revival. It is attractive that when $r = 0.5$ and $p = 1/\sqrt{2}$ (Werner case), the LQU is more robust than entanglement. Indeed, our numerical analysis corroborates the results reported in Refs [53–55]. In fact the authors showed that that for all states, with non zero discord, the interaction with any Markovian bath can never lead to a sudden and permanent vanishing of discord and the entanglement sudden death phenomenon is then explained by the existence of separability.

Figure 3e shows that the inhomogeneous magnetic files b have a destructive effect on the quantum correlations. When the system is initially prepared in the mixed state Fig. 3f, the concurrence and LQU are not symmetric relative to $b = 0$. The height of the amplitude of these functions considerably decreases as $|b|$ increases. When $b > 0$, the concurrence exhibits a death and revival process for a certain interval of b. Then for large values of $|b|$ indicates the phenomenon of entanglement sudden death. In the negative range of b, the concurrence oscillates gradually as $|b|$ decrease and then suddenly disappears. The LQU continues with tiny oscillations without death and revival phenomena until the system reaches a steady state at a value very close to zero. Besides, the bipartite quantum correlations are more robust in the region when $b < 0$. This is due to the fact that in the negative regimes of the external inhomogeneous magnetic field, the relative effects will be such that the correlations between the sub-systems of the composite state are disturbed the least as compared to that in the positive regimes of the field. Thus, the optimal value of the magnetic field strength where the system remains more correlated is $b < 0$. This sudden change in quantum correlations behavior in the two-qubits state can be used to achieve optimal procedure for choosing the measurement operators [56,57] to investigate specific regions of interest where the system will remain less disturbed and thus more correlated. In the case when the system is initially prepared in the mixed state, we observed less deformation in quantum correlations in the two-qubits system in the region $b < 0$. Therefore, Fig. 3 shows the destructive effect of the inhomogeneous magnetic field b on the correlations of the system. This behavior is predictable since the dynamics of the concurrence and LQU are severely affected by the inhomogeneous magnetic field and intrinsic decoherence which play a negative role in inhibiting decoherence. Very particularly, the external degree of freedom (magnetic field, environment coupling) degrades the property of the quantum system.

In Fig. 4, the LQFI is plotted against the spin interaction strength parameter J including: the anti-ferromagnetic range ($J > 0$) and ferromagnetic range ($J < 0$) and also versus the degree the field inhomogeneity b. Similarly to the LQU and concurrence behaviors, in the first region ($J < 0$) the LQFI decreases gradually to reaches its minimum values at $J = 0$, while in the second region ($J > 0$), it increases suddenly to achieve again the maximum value for large numbers of J. However, the oscillating behavior of quantum correlations appears only for maximally entangled state, namely $r = 1$ and $p = \frac{1}{\sqrt{2}}$ (See Fig. 4a, d), while for the Werner state ($p = \frac{1}{\sqrt{2}}$), then the oscillation correlations disappears totally. However, the evolution of LQFI against the parameter b is given in the plots Fig. 4d–f. Obviously, in the case of a maximally entangled state (Fig. 4d), the plot shows many the oscillations of correlations. Roughly speaking, in the first region, namely ($b < 0$) the amount of LQFI are reduced asymptotically from its
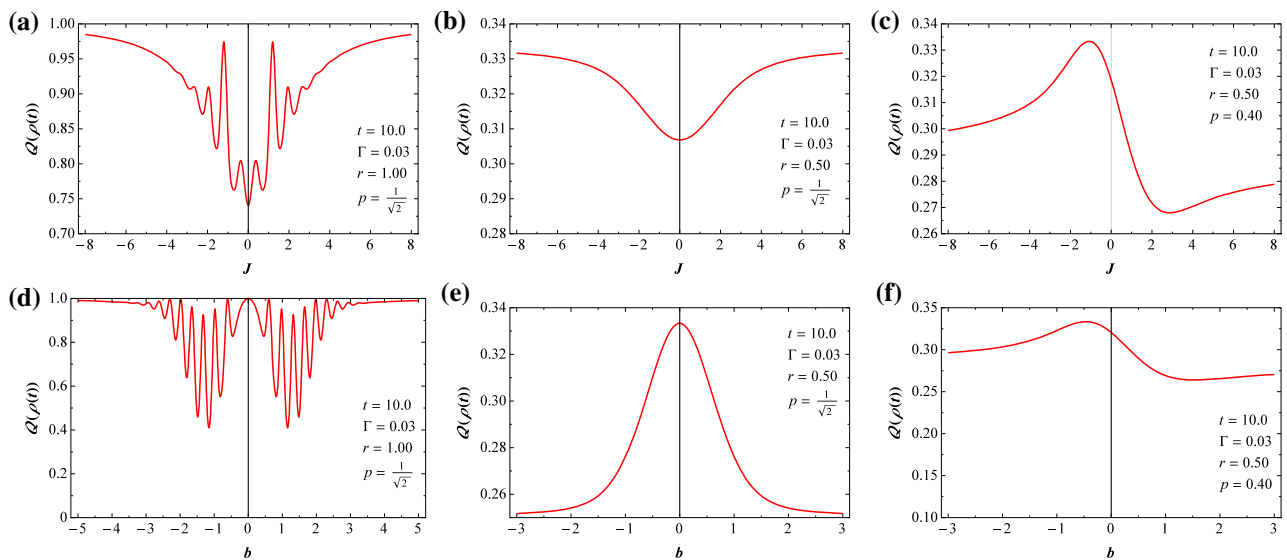
Fig. 4 Upper panels: dynamics of local quantum Fisher information as a function of the exchange coupling parameter J when the system is initially prepared in the maximally entangled state (**a**), in the Werner state (**b**), and in the mixed state (**c**), taking $b = 0.20$, $t = 10$ and $\Gamma = 0.03$. Lower panels: dynamics of local quantum Fisher information as a function of the inhomogeneous magnetic field b when the system is initially prepared in the maximally entangled state (**d**), in the Werner state (**e**), and in the mixed state (**f**), taking $J = 1$, $t = 10$ and $\Gamma = 0.03$

Table 1 A comparative study between LQU, LQFI, and concurrence

| Initial states	Sudden death	Sudden birth	Oscillations correlations	Frozen correlations
Pure state	LQU	None	LQU, C and LQFI	LQU, C and LQFI
Werner state	LQU and C	LQU and C	LQU and C	LQU, C and LQFI
Maximally entangled state	LQU	LQU, C and LQFI	LQU, C and LQFI	LQU, C and LQFI
Mixed state	LQU and C	LQU and C	LQU, C and LQFI	LQU, C and LQFI

maximum bound and suddenly increases to achieve again the maximum value for $b = 0$. In the second region, namely $b > 0$ the LQFI decreases gradually and achieve the maximum peak for large numbers of the parameter b. Again in the case of Werner state, the oscillations of the correlations and sudden-death phenomena don't occur and the maximum correlations are obtained around $b = 0$. The frozen LQFI phenomenon occurs for small values of p (See Fig. 4f). As it can be seen from this figure, the LQFI bounds are always greater than LQU and concurrence. From the discussion above, we conclude that the exchange coupling parameter induces quantum correlations between two qubits in contrast to the inhomogeneous magnetic field as well as the intrinsic decoherence rate loss of the quantum correlations. This means that there exists a competition between the Heisenberg exchange coupling coefficient and the inhomogeneous magnetic field as well as the intrinsic decoherence.

The influences of the initial states, the exchange coupling parameter, inhomogeneous magnetic field, and the intrinsic decoherence rate on the dynamics of non-classical correlations have been investigated in detail. Our findings show that the dynamics of the entanglement termed by the concurrence, local quantum uncertainty, and local quantum Fisher information are strongly dependent on the forms of initial states. Our numerical results corroborate the results reported in [34,58]. When the system is initially prepared in a Werner-like state (10), the dynamical behaviors of these quantum correlation measures are independent of the external magnetic field B and the exchange anisotropy parameter Δ. The dynamical behaviors of the mentioned quantifiers exhibit damped oscillations with respect to time. While for initial product state (i.e., $\rho(0) = |01\rangle \langle 01|$), the concurrence and LQU can be created due to the spin–spin coupling interaction.

The following Table 1 summarizes the four generated phenomena already pointed out, namely sudden death, sudden birth, oscillation correlations, and frozen correlations phenomena in the case pure, Werner, maximally entangled, and mixed states.

Finally, since the density operator $\rho(t)$ is an entangled and maximally entangled state for some critical values of t, b and J, namely $t = 0$ and large numbers of J and b, then it would be very motivated to consider it as a quantum channel in order to implement a protocol of quantum teleportation under local-time dynamics and in the presence of intrinsic decoherence effect. In this sense, we shall examine in the next session the non-classical correlations by means of LQFI and LQU and the entanglement measure in terms of concurrence of the teleported state, namely $\rho_{out}(t)$ given by Eq.(47).

Fig. 5 The scheme of quantum teleportation using $\rho(t)$ as an entangled partial source, where U is the unitary operation required to restore the input state $\rho_{\text{in}}(t)$. The teleported output state is denoted by $\rho_{\text{out}}(t)$
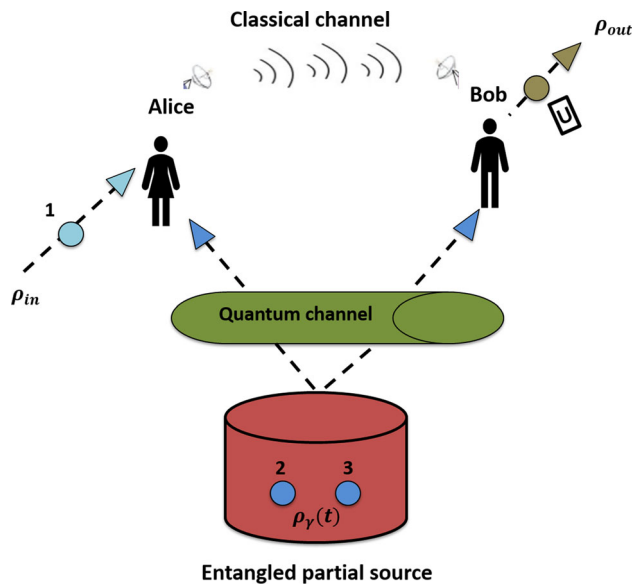
5 Quantum teleportation

In this section, we implement a scheme of quantum teleportation using, as a resource, an entangled mixed state. Indeed, according to Bowen et al [59–61], the scheme of quantum teleportation with arbitrary two-qubit mixed states can be regarded as a general depolarizing quantum channel. The significant results of this work are shown in the ability to take into account the mixed teleported states, except in the case of a maximally entangled channel. Next, we investigate the effects of the intrinsic decoherence phenomenon on the transmission of information shared between a two-partners, namely Alice and Bob using the obtained density operator $\rho(t)$ in Eq.(14) as a quantum channel (See Fig. 5). Assume that the input state being the following arbitrary unknown two-qubit pure state $||\psi_{in}\rangle\rangle$

$$||\psi_{\text{in}}\rangle\rangle = \cos\left(\frac{\theta}{2}\right)||10\rangle\rangle + e^{i\phi}\sin\left(\frac{\theta}{2}\right)||01\rangle\rangle, \tag{44}$$

where $\theta \in [0, \pi]$ and $\phi \in [0, 2\pi]$ denote the amplitude and the phase of the input state, respectively. After some straightforward calculations, the concurrence of the input state $\rho_{in} = ||\psi_{in}\rangle\rangle\langle\langle\psi_{in}||$ turns out to be

$$\mathcal{C}_{\text{in}} = |\sin(\theta)|. \tag{45}$$

From the mathematical point of view, the quantum channel is known as a completely positive and trace-preserving operator. Via this mechanism, an input density operator is mapped to an output density operator [59–61]. When the quantum state is teleported through the mixed channel ρ_{ch}, the output replica state ρ_{out} can be obtained by applying a joint measurement and local unitary transformation to the input state ρ_{in} [59–62], hence

$$\rho_{\text{out}} = \sum_{\mu,\nu=0}^{3} p_{\alpha\beta}(\sigma^{\mu} \otimes \sigma^{\nu})\rho_{\text{in}}(\sigma^{\mu} \otimes \sigma^{\nu}), \tag{46}$$

where $\sigma^0 = I$ (I defining 2×2 identity matrix). The joint probabilities are $p_{\mu\nu} = p_{\mu}p_{\nu}$, where $p_{\mu} = \text{Tr}(E^{\mu}\rho(t))$ satisfy the condition $\sum_{\mu,\nu} p_{\mu\nu} = 1$. The projective measurements are defined by; $E^0 = ||\Psi^-\rangle\rangle\langle\langle\Psi^-||$, $E^1 = ||\Phi^-\rangle\rangle\langle\langle\Phi^-||$, $E^2 = ||\Psi^+\rangle\rangle\langle\langle\Psi^+||$, and $E^3 = ||\Phi^+\rangle\rangle\langle\langle\Phi^+||$, where $\{||\Psi^{\pm}\rangle\rangle, ||\Phi^{\pm}\rangle\rangle\}$ are the well-known Bell states. Therefore, the density operator of the output state ρ_{out} can be calculated straightforwardly from Eq.(46). Indeed, it takes the following matrix form

$$\rho_{\text{out}}(t) = \begin{pmatrix} \widetilde{\rho}_{11}(t) & 0 & 0 & 0 \\ 0 & \widetilde{\rho}_{22}(t) & \widetilde{\rho}_{23}(t) & 0 \\ 0 & \widetilde{\rho}_{23}^*(t) & \widetilde{\rho}_{33}(t) & 0 \\ 0 & 0 & 0 & \widetilde{\rho}_{11}(t) \end{pmatrix}, \tag{47}$$

where

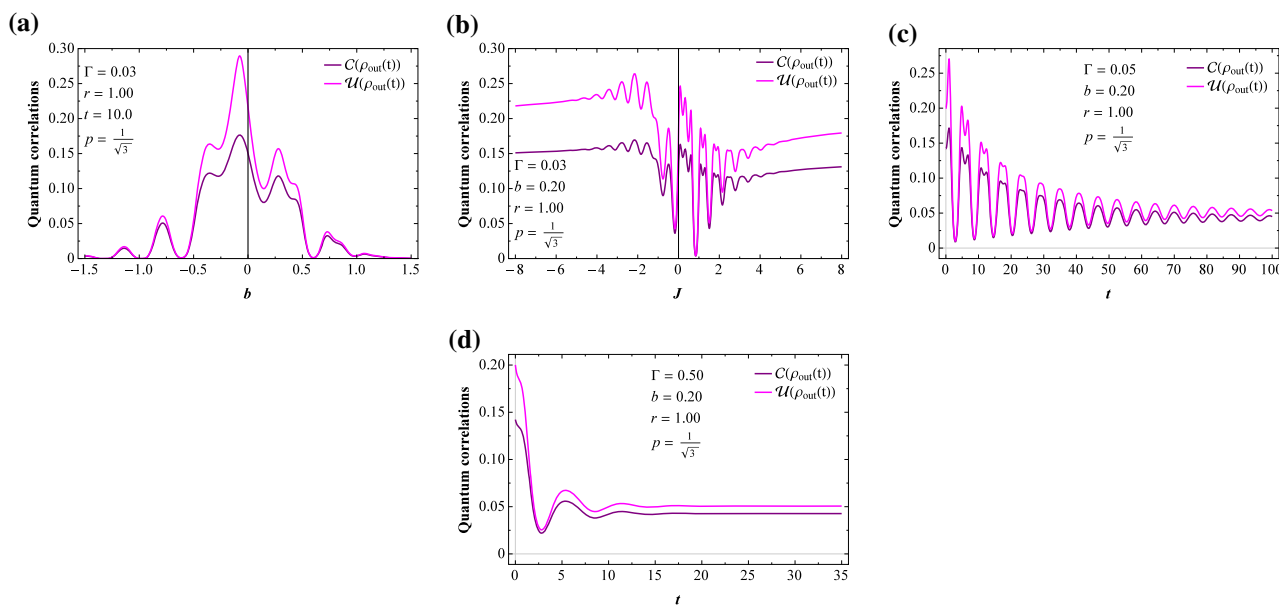$$\widetilde{\rho}_{11}(t) = (\rho_{11}(t) + \rho_{44}(t))(\rho_{22}(t) + \rho_{33}(t)),$$

Fig. 6 The dynamics of quantum correlation quantifiers for the output state ρ_{out} versus the inhomogeneous magnetic field b for the parameter set $J = 1$, $t = 10$, and $\Gamma = 0.03$ when the system is initially prepared in the pure state (**a**). The exchange coupling dependence of the dynamics of quantum correlation and fixed $b = 0.20$. The same quantifiers as a function of the time parameter t by assuming $J = 1$ and $b = 0.20$ when $\Gamma = 0.05$ (**c**) and $\Gamma = 0.5$ (**d**)

$$\widetilde{\rho}_{22}(t) = (\rho_{11}(t) + \rho_{44}(t))^2 \cos^2\left(\frac{\theta}{2}\right) + (\rho_{22}(t) + \rho_{33}(t))^2 \sin^2\left(\frac{\theta}{2}\right),$$

$$\widetilde{\rho}_{33}(t) = (\rho_{11}(t) + \rho_{44}(t))^2 \sin^2\left(\frac{\theta}{2}\right) + (\rho_{22}(t) + \rho_{33}(t))^2 \cos^2\left(\frac{\theta}{2}\right),$$

$$\widetilde{\rho}_{23}(t) = 2e^{i\phi}\rho_{23}(t)\sin\theta.$$

We first consider the dynamical evolution of quantum correlations quantifiers of the output state ρ_{out}, i.e., concurrence $\mathcal{C}(\rho_{\text{out}})$ and $\mathcal{U}(\rho_{\text{out}})$ when the system is in the pure entangled state ($r = 1$ and $p = 1/\sqrt{3}$) for fixed $J = 1$ and $\Delta = 0.5$ which are presented in Fig. 6. We plot in Fig. 6a the above-mentioned quantum correlations quantifiers as functions of the inhomogeneous magnetic field for $t = 10$. Both quantifiers have the same behavior, namely, they decrease from a typical maximum with the increase of $|b|$. The phenomena of sudden death and growth of entanglement also occur in the behavior of the concurrence and LQU in the output state. For higher values of the inhomogeneous magnetic field $|b|$, the output concurrence and LQU vanish indicating that there are no quantum correlations (the information between two-qubit is destroyed). Thus, in this situation ($|b| < 0.5$), the concurrence and LQU of the teleported state reach large amplitudes which are good for the success of the quantum teleportation protocol. However, for a sufficiently strong inhomogeneous magnetic field, the output concurrence and LQU gradually decrease, and the entangled state teleportation will not succeed anymore. We plot in Fig. 6b the concurrence and LQU versus the exchange coupling parameter J for $b = 0.20$. The quantum correlations in the output state behave like the results shown for the input state in Fig. 3c. Besides, as $|J|$ increases, both quantifiers oscillate with a tendency to reach a steady state. The frozen phenomenon appears in the output state, which means that information between two-qubit is secured. The output quantum correlations in the ferromagnetic phase predominate over the antiferromagnetic phase. From Fig. 6c, d, the effect of intrinsic decoherence rate is clearly seen through the oscillating behavior of the correlations as a function of time with large amplitudes for LQU. The sudden death phenomenon can be prevented by increasing Γ and at the early times lead to the same steady-state values of the correlations depicted in Fig. 6c. On the other hand, these results are compatible with the results in Fig. 1a for the input state, except that for the teleported state the LQU captures more information than concurrence. Further, we notice that quantum teleportation can be improved by increasing the intrinsic parameter Γ. Thus, we conclude that parameter Γ is an efficient control parameter of quantum communications. This is illustrated in Fig. 6d. According to our numerical calculations, we conclude that the LQU is more robust than concurrence for either input states or output states. In general, the LQU is a discord-like measure of quantum correlations this explains the robustness in comparison with the entanglement (concurrence) [46]. In this sense, LQU has a relevant application in the field of quantum metrology and quantum information processing. Therefore, it is desirable to investigate, characterize, and quantify quantum correlations more broadly.

Figure 7 examines the LQFI as a measure of non-classical correlations of the teleported state. It is clear that the teleported LQFI shows many oscillations for various values of b and r and the increase of the decoherence parameter, namely Γ allows to enhance the LQFI of the teleported state. Moreover, the frozen teleported LQFI appears again for some special values of J, b and
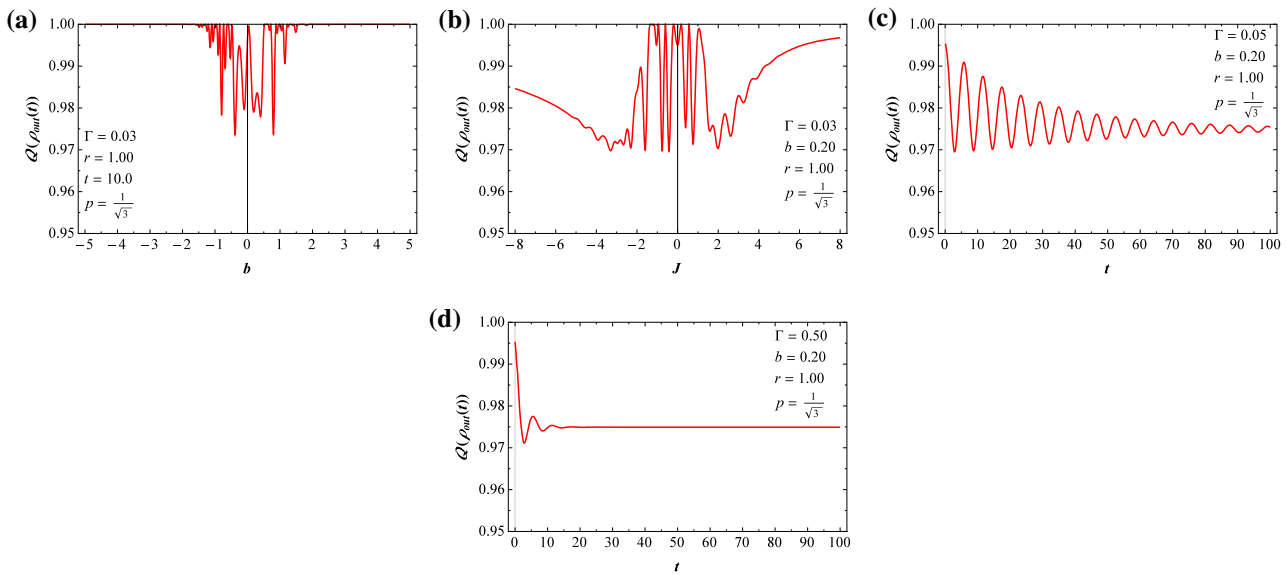
Fig. 7 The dynamics of local fisher information for the output state ρ_{out} versus the inhomogeneous magnetic field b for the parameter set $J = 1$, $t = 10$, and $\Gamma = 0.03$ when the system is initially prepared in the pure state (**a**). The exchange coupling dependence of the dynamics of LQU and fixed $b = 0.20$. The same quantifiers as a function of the time parameter t by assuming $J = 1$ and $b = 0.20$ when $\Gamma = 0.05$ (**c**) and $\Gamma = 0.5$ (**d**)

t. Moreover, it appears fast in the case when Γ takes large values (See Fig. 7d) which indicates an emerging future of frozen LQFI under teleportation protocol in the presence of intrinsic decoherence effects.

6 The fidelity of entanglement teleportation

In order to estimate the quality teleportation process, it is often quite useful to study the fidelity between ρ_{in} and ρ_{out} to characterize the transmission credibility of the secure information shared between Alice and Bob. We note that when the input state is a pure state, we can apply the concept of fidelity as a useful indicator of the teleportation performance of a quantum channel [63]. The fidelity is determined by

$$\mathcal{F} = \left(\text{Tr} \sqrt{ \sqrt{\rho_{\text{in}}} \rho_{\text{out}} \sqrt{\rho_{\text{in}}} } \right)^2, \tag{48}$$

We note that the fidelity is near zero if the input and the output state are orthogonal which implying that the information is completely destroyed during the transmission process and the teleportation fails. While it is close to unity if the input state and the output state are identical. In the case when $0 < \mathcal{F} < 1$ the quantum information is subjected to distortions after transmitting to some extent. Using Eq.(47), after a straightforward calculation, the fidelity is given by

$$\mathcal{F} = \frac{\sin^2 \theta}{2} [(\rho_{11}(t) + \rho_{44}(t))^2 + 4\rho_{23}^2(t) - (\rho_{22}(t) + \rho_{33}(t))^2] + (\rho_{22}(t) + \rho_{33}(t))^2. \tag{49}$$

Since the parameters θ and ϕ are unknown, we calculate the average of the fidelity $\mathcal{F}_A$ over all the points of Bloch sphere. This is given by

$$\mathcal{F}_A = \frac{1}{4\pi} \int_0^{2\pi} d\phi \int_0^\pi d\theta \mathcal{F} \sin \theta, \tag{50}$$

which gives

$$\mathcal{F}_A = \frac{1}{3} [(\rho_{11}(t) + \rho_{44}(t))^2 + 4\rho_{23}^2(t) + 2(\rho_{22}(t) + \rho_{33}(t))^2]. \tag{51}$$

Obviously, the average fidelity $\mathcal{F}_A$ depends basically on the quantum channel parameters. To transmit the input state $|\psi_{\text{in}}\rangle$ with better fidelity than any classical communication protocol, $\mathcal{F}_A$ must exceed $\frac{2}{3}$, which is the maximum achievable for classical communication. Figure 8a, b shows the average fidelity against the exchange coupling parameter in the pure state and mixed state, respectively, for mixed values of $b = 0.20$, $\Gamma = 0.03$, and for $t = 10$ where several fixed values of the purity have been considered.
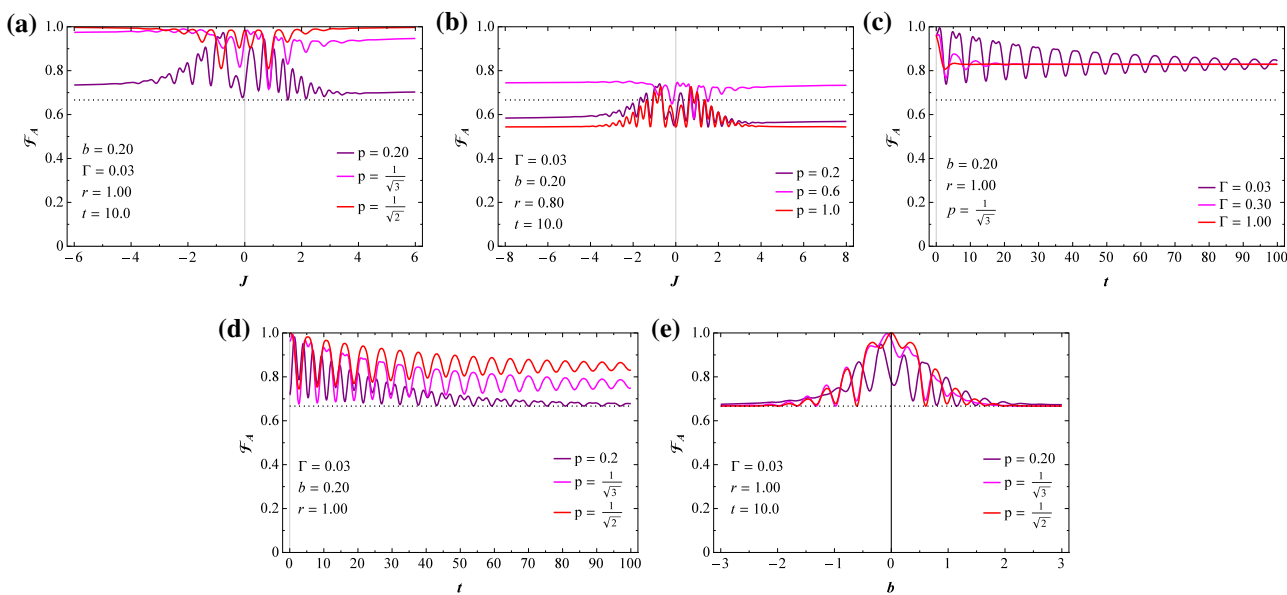
Fig. 8 $\mathcal{F}_A$ versus the exchange coupling coefficient, assuming $b = 0.20$, $t = 10$, and $\Gamma = 0.03$ and several fixed values of the degree of entanglement p, when the system is initially prepared in the pure state (**a**), in the mixed state (**b**). The time dependence of the average fidelity for various values of the intrinsic decoherence parameter (**c**), and the degree of entanglement parameter (**d**), where other parameters have taken as $b = 0.20$ and $r = 1$. $\mathcal{F}_A$ against the inhomogeneous magnetic field b when different fixed values of the magnetic field are considered such that $\Gamma = 0.03$ and $r = 1$

In these figures, the horizontal dashed lines at $\mathcal{F}_A = \frac{2}{3}$ denote the limit of quantum fidelities. When the system is initially prepared in the pure state ($r = 1$) (Fig. 8a), the average fidelity shows many oscillations as the parameter p decreases. Moreover, all curves eventually reach a steady state as the exchange coupling parameter increases, which means that the amount of average fidelity is frozen for a certain time. The inclusion of purity stimulates an increase in the average fidelity until reaching maximum fidelity ($\mathcal{F}_A = 1$). It is also observed that the quantum communication is enhanced with the increase of $|J|$ ($\mathcal{F}_A > 2/3$ represented as a dash-dotted line). In Fig. 8b, the plot shows that the teleportation will not succeed for $\mathcal{F}_A < 2/3$, because the system is initially in the interphase between the entangled state and the separable state in contrast to the situation when the system is prepared in the pure state Fig. 8a, the success of the teleportation depends on the purity parameter. For example, when $r = 0.80$ and $p = 0$, we have a dramatic increase of average fidelity and at lower values of the spin coupling, it reaches the maximum value and then decreases monotonically below $2/3$ as soon as $|J|$ increases. The average fidelity $\mathcal{F}_A$ remains below $2/3$, making it impossible for the existence of quantum teleportation of the information. In Fig. 8c, the evolution of the average fidelity $\mathcal{F}_A$ is plotted for certain values of the intrinsic decoherence parameter when the system is prepared in the pure state. As we can see, the average fidelity oscillates over time and reaches a stable value when time t approaches infinity. Larger the parameter Γ, while the shorter one is the time of reaching the stable values Fig. 8c. Moreover, the stable value remains always above $2/3$, which means that such teleportation through the two-qubit Heisenberg XXZ model is better than any classical communication protocol. When the system is in the initial pure state, the behavior of the average fidelity becomes more robust, enabling the teleportation of information in the regions of large value of intrinsic rate ($\Gamma = 1$). Therefore, the initial state and the parameters of the model are significant factors to determine what kinds of systems are suitable as a quantum channel. From these figures, we can see that the fidelity can reach the unity for $p = 1/\sqrt{2}$, which means that the channel is the two-qubit maximally entangled state, namely $|\phi\rangle = \frac{1}{\sqrt{2}}(|01\rangle + |10\rangle)$, and two-qubit states can always be teleported with a pair of EPR states which agrees with the results reported in [64]. Figure 8e shows the effects of the inhomogeneous magnetic field on the average fidelity when the system is initially prepared in a Bell-like state. The average fidelity achieves the maximum amount at $b = 0$ then gradually decreases as b increases to a critical value of $2/3$. The decay of the average fidelity as a function of b means that the inhomogeneous magnetic field b has unfortunately a destructive effect on the average fidelity. As a result, one conclude that the initial-parameters state of the channel plays an important role in the average fidelity of teleportation. It is found that when the initial state is entangled state $|\phi\rangle = \alpha|01\rangle + \beta|10\rangle$ the corresponding average fidelity is always larger than $2/3$ (a similar behavior was reported by N. Zidan in Ref. [58]).

7 Conclusions

In this work, we have demonstrated a straightforward analysis of the dynamics of a two-qubit system on the Heisenberg XXZ model under intrinsic decoherence. We first assumed that the system interacts with an external magnetic field, B with only nearest-neighbor

interactions. After exactly solving the time-independent master equation, we have investigated the dynamics of the concurrence, local quantum uncertainty and local quantum Fisher information in order to quantify the quantum correlations of this system. We have concluded that all these quantifiers oscillate similarly between their upper and lower bounds where in general the LQFI is more stable comparing to the LQU and concurrence. The sudden death, sudden birth, oscillations, and frozen correlations phenomena appear clearly for different initial settings. By making a comparative study between the dynamics of $\mathcal{C}$, LQU and LQFI, we have obtained some interesting outcomes. For example, the intrinsic decoherence destroys the oscillations of the correlations between the qubits. For the initially mixed state, we have concluded that the dynamics under intrinsic decoherence causes the sudden death phenomenon for some particular initial state settings, while both LQU and LQFI quantities resist the decoherence effect. This implies that the absence of entanglement does not necessarily mean the absence of non-classical correlations in the quantum states. Besides, the robustness and the generation of the quantum correlations depend on the physical parameters and the initial state as well. Further, our investigations emphasize that efficient information processing based on the LQU and LQFI offers more resistance to the effect of intrinsic decoherence and is completely different from the entanglement. Finally, we have examined the possibility of teleportation process through the model under consideration. We have showed that when the system is initially prepared in entangled state, the corresponding average fidelity is always larger than 2/3, which means the success of the teleportation in contrast to the case when the system is initially in the interphase between the entangled state and the separable state. Indeed, the initial state of the channel plays an important role in the fully entangled fraction and the average fidelity of teleportation. In particular, we showed that the average fidelity achieves the maximum amount when the degree of inhomogeneity of the field vanishes. Moreover, large numbers of the decoherence parameter allow to enhance different quantities, namely teleported concurrence, LQU, LQFI, and fidelity. Therefore, one can conclude that different parameters encoded in the two-qubit Heisenberg XXZ model are an efficient control parameter of quantum communications.

In summary, it is possible to prepare an entangled mixed state arising from the interaction between a two-qubit open systems interacting with its environments under Markovian dynamics. These results can be used analytically and experimentally in many areas of secure communication, quantum information theory and quantum estimation theory. Our future perspective will concern other types of environments in order to investigate the crucial relationship between entanglement, LQU and LQFI in Markovian and also non-Markovian regimes and to extend the present work higher dimensional. Moreover, it will be motivated for us to take into account the influence of Dzyaloshinski–Moriya interaction on the dynamics of entanglement and quantum correlations. Indeed, in this context, Y-n. Guo et al [34] quantifies the quantum correlations by means of LQU of a two-qubit one-dimensional XYZ Heisenberg chain with Dzyaloshinski–Moriya interaction in thermal equilibrium, where interestingly enough they showed that for an initial separable state, the quantum correlations by means of LQU can be induced due to the Dzyaloshinski–Moriya interaction and Heisenberg anisotropic interaction.

References

1. A. Datta, A.T. Flammia, C.M. Caves, Entanglement and the power of one qubit. Phys. Rev. A **72**, 043216 (2005)
2. A. Datta, G. Vidal, Role of entanglement and correlations in mixed-state quantum computation. Phys. Rev. A **75**, 042310 (2007)
3. F. Benabdallah, A. Slaoui, M. Daoud, Quantum discord based on linear entropy and thermal negativity of qutrit-qubit mixed spin chain under the influence of external magnetic field. Quantum Inf. Process. **19**, 252 (2020)
4. M.A. Nielsen, I.L. Chuang, *Quantum Computation and Quantum Information* (Cambridge University Press, Cambridge, 2000)
5. M. Le Bellac, *A Short Introduction to Quantum Information and Quantum Computation* (Cambridge University Press, Cambridge, 2006)
6. A. Streltsov, H. Kampermann, S. Wölk, M. Gessner, D. Bruß, Efficient quantum state analysis and entanglement detection. New J. Phys. **20**, 053058 (2018)
7. A. Streltsov, G. Adesso, M.B. Plenio, Colloquium: quantum coherence as a resource. Rev. Mod. Phys. **89**, 041003 (2017)
8. C.H. Bennett, G. Brassard, C. Crepeau, R. Jozsa, A. Peres, W.K. Wootters, Teleporting an unknown quantum state via dual classical and Einstein–Podolsky–Rosen channels. Phys. Rev. Lett. **70**, 1895 (1993)
9. H.L. Huang, Quantum teleportation via a two-qubit Ising Heisenberg chain with an arbitrary magnetic field. Int. J. Theor. Phys. **50**, 70–79 (2011)
10. G.C. Fouokeng, E. Tedong, A.G. Tene, M. Tchoffo, L.C. Fai, Teleportation of single and bipartite states via a two qubits XXZ Heisenberg spin chain in a non-Markovian environment Phy. Lett. A **384**, 126719 (2020)
11. A.K. Ekert, Quantum cryptography based on Bell's theorem. Phys. Rev. Lett. **67**, 661 (1991)
12. C.H. Bennett, S.J. Wiesner, Communication via one- and two particle oprators on Einstein–Podolsky–Rosen states. Phys. Rev. Lett. **69**, 20 (1992)
13. R. Horodecki, P. Horodecki, M. Horodecki, K. Horodecki, Quantum etanglement. Rev. Mod. Phys. **81**, 865 (2009)
14. V. Vedral, The role of relative entropy in quantum information theory. Rev. Mod. Phys. **74**, 197 (2002)
15. O. Gühne, G. Tóth, Entanglement detection. Phys. Rep. **474**, 1 (2009)
16. K. Modi, A. Brodutch, H. Cable, T. Paterek, V. Vedral, The classical-quantum boundary for correlations: discord and related measures. Rev. Mod. Phys. **84**, 1655 (2012)
17. W.K. Wootters, Entanglement of formation for an arbitrary state of two qubits. Phys. Rev. Lett. **80**, 10 (1998)
18. D. Girolami, T. Tufarelli, G. Adesso, Characterizing nonclassical correlations via local quantum uncertainty. Phys. Rev. Lett. **110**, 240402 (2013)
19. M. Ali, Local quantum uncertainty for multipartite quantum systems. Eur. Phys. J. D **74**, 186 (2020)
20. E.P. Wigner, M.M. Yanasse, Informations contents of distributions. Proc. Nat. Acad. Sci. USA **19**, 910 (1963)
21. S. Luo, Using measurement-induced disturbance to characterize correlations as classical or quantum. Phys. Rev. A **77**, 022301 (2008)
22. S. Luo, Wigner–Yanase skew information and uncertainty relations. Phys. Rev. Lett. **91**, 180403 (2003)
23. S. Luo, Wigner–Yanase skew information vs. quantum fisher information. Proc. Am. Math. Soc. **132**, 885 (2003)
24. D. Petz, C. Ghinea, Introduction to quantum fisher information. Quantum Probab. Relat. Top. **1**, 261–281 (2011)

25. Y. Akbari-Kourbolagh, M. Azhdargalam, Entanglement criterion for multipartite systems based on quantum Fisher information. Phys. Rev. A **99**, 012304 (2019)

26. S. Haseli, Local quantum Fisher information and local quantum uncertainty in two-qubit Heisenberg XYZ chain with Dzyaloshinskii–Moriya interactions. Laser Phys. **30**, 105203 (2020)

27. A.B.A. Mohamed, E. Khalil, M.M. Selim, H. Eleuch, Quantum Fisher information and bures distance correlations of coupled two charge-qubits inside a coherent cavity with the intrinsic decoherence. Symmetry **13**, 2 (2021)

28. X. Hu, H. Fan, D.L. Zhou, W.-M. Liu, Necessary and sufficient conditions for local creation of quantum correlation. Phys. Rev. A. **85**, 032102 (2012)

29. F. Benabdallah, M. Daoud, Dynamics of quantum discord based on linear entropy and negativity of qutrit–qubit system under classical dephasing environments. Eur. Phys. J. D **75**, 3 (2021)

30. F. Benabdallah, H. Arian Zad, M. Daoud and N. Ananikian, Dynamics of quantum correlations in a qubit-qutrit spin system under random telegraph noise, Phys. Scr. **96** 125116 (2021)

31. K. El Anouz, A. El Allati, N. Metwally, Different indicators for Markovian and non-Markovian dynamics. Phy. Lett. A. **384**, 5 (2019)

32. A.-B.A. Mohamed, N. Metwally, Non-classical correlations based on skew information of entangled two qubit-system with non-mutual interaction under a intrinsic decoherenc. Ann. Phys. **381**, 137–150 (2017)

33. V. Abhignan, R. Muthuganesan, Effects of intrinsic decoherence on discord-like correlation measures of two-qubit spin squeezing model. Phys. Scr. **96**, 125114 (2021)

34. Y.-N. Guo, H.-P. Peng, Q.-L. Tian, Z.-G. Tan, Y. Chen, Local quantum uncertainty in a two-qubit Heisenberg spin chain with intrinsic decoherence. Phys. Scr. **96**, 075101 (2021)

35. A.B.A. Mohamed, A.H. Abdel-Aty, E.G. El-Hadidy, H.A.A. El-Saka, Two-qubit Heisenberg XYZ dynamics of local quantum Fisher information, skew information coherence: Dyzaloshinskii–Moriya interaction and decoherence. Results Phys. **30**, 104777 (2021)

36. L-P. Chen, Y-n. Gu, Dynamics of local quantum uncertainty and local quantum fisher information for a two-qubit system driven by classical phase noisy laser, J. Mod. Opt. **68**, 4 (2021)

37. B.-L. Ye, B. Li, X.-B. Liang, S.-M. Fei, Dynamics of local quantum uncertainty and local quantum Fisher information for a two qubit system driven by classical phase noisy laser. Inte J. Quatum Inf. **18**, 04 (2020)

38. G. Najarbashi, Seifi, B, Quantum phase transition in the Dzyaloshinskiiâ€Moriya interaction with inhomogeneous magnetic field: Geometric approach. Quantum Inf. Process. **16**, 40 (2017)

39. A. Karlsson, M. Bourennane, Quantum teleportation using three-particle entanglement. Phys. Rev. A. **58**, 4394 (1998)

40. J.C. Hao, C.F. Li, G.C. Guo, Controlled dense coding using the Greenberger–Horne–Zeilinger state. Phys. Rev. A. **63**, 054301 (2001)

41. A.-Z. Hamid, M. Hossein, Transferring information through a mixed-five-spin chain channel. Chin. Phys. B. **25**, 080307 (2016)

42. G. Milburn, Intrinsic decoherence in quantum mechanics. Phys. Rev. A **44**(9), 5401 (1991)

43. R.F. Werner, Quantum states with Einstein–Podolsky-Rosen correlations admitting a hidden-variable model. Phys. Rev. A **40**, 4277 (1989)

44. M. Asoudeh, V. Karimipour, Thermal entanglement of spins in an inhomogeneous magnetic field. Phys. Rev. A **71**, 022308 (2005)

45. M. Berman, R. Kosloff, H. Tal-Ezer, Solution of the time-dependent Liouville-von Neumann equation: dissipative evolution. J. Phys. A Math. Gen. **25**, 1283 (1992)

46. M. Ali, A.R.P. Rau, G. Alber, Quantum discord for two-qubit X states. Phys. Rev. A **81**, 042105 (2010)

47. C.W. Helstrom, *Quantum Detection and Estimation Theory* (Academic, New York, 1976)

48. G.A. Matteo, Paris, "Quantum estimation for quantum technology." Int. J. Quant. Inf. **7**, 125 (2009)

49. S.L. Braunstein, C.M. Caves, Statistical distance and the geometry of quantum states. Phys. Rev. Lett. **72**, 3439 (1994)

50. S. Kim, L. Li, A. Kumar, J. Wu, Characterizing nonclassical correlations via local quantum Fisher information. Phys. Rev. A. **97**, 032326 (2018)

51. K. El Anouz, I. El Aouadi, A. El Allati and T. Mourabit, Dynamics of quantum correlations in quantum teleportation, International Journal of Modern Physics B **34**, 10 2050093 (2020)

52. J.L. Guo, H.S. Song, Effects of inhomogeneous magnetic field on entanglement and teleportation in a two-qubit Heisenberg XXZ chain with intrinsic decoherence. Phys. Scr. **78**, 045002 (2008)

53. A. Ferraro, D. Cavalcanti, F.M. Cucchietti, A. Acín, Phys. Rev. A **81**, 052318 (2010)

54. K. Zyczkowski, P. Horodecki, A. Sanpera, M. Lewenstein, Phys. Rev. A **58**, 883 (1998)

55. S.L. Braunstein, C.M. Caves, R. Jozsa, N. Linden, S. Popescu, R. Schack, Phys. Rev. Lett. **83**, 1054 (1999)

56. T. Werlang, G. Rigolin, Thermal and magnetic quantum discord in Heisenberg models. Phys. Rev. A **81**, 044101 (2010)

57. J. Yang, Y. Huang, Tripartite and bipartite quantum correlations in the XXZ spin chain with three-site interaction. Quantum Inf. Process. **16**, 281 (2017)

58. N, Zidan, Quantum teleportation via two-qubit Heisenberg XYZ chain, Can. J. Phys. **92**, 406 (2014)

59. G. Bowen, S. Bose, Teleportation as a depolarizing quantum channel, relative entropy, and classical capacity. Phys. Rev. Lett. **87**, 267901 (2001)

60. Y. Yeo, Teleportation via thermally entangled states of a two-qubit Heisenberg XX chain, Phys. Rev. A **66**, 062312

61. Y. Zhou, G.F. Zhang, Quantum teleportation via a two-qubit Heisenberg XXZ chain-effects of anisotropy and magnetic field. Eur. Phys. J. D **47**, 227 (2008)

62. A. Peres, Separability criterion for density matrices. Phys. Rev. Lett. **77**, 1413 (1996)

63. R. Jozsa, Fidelity for mixed quantum states. J. Mod. Opt. **41**, 12 (1994)

64. L. Qiu, A.M. Wang, X.Q. Su, Effect of Dzyaloshinskill–Moriya anisotropic antisymmetric interaction and intrinsic decoherence on entanglement teleportation. Physica A **387**, 6686 (2008)